Mercury intrusion porosimetry of plasma-sprayed ceramic

J. ILAVSKY*
Ceramics Group, National Institute of Standards and Technology, Gaithersburg, MD 20899, USA

C. C. BERNDT‡, J. KARTHIKEYAN‡
The Thermal Spray Laboratory, State University of New York at Stony Brook, Stony Brook, NY 11794–2275, USA

Limitations and corrections for the application of mercury intrusion porosimetry (MIP) in measuring plasma-sprayed ceramic (alumina–titania) deposits are studied. The data reduction procedures of the MIP technique are discussed; the importance of which changes between different machines and samples. Thus, it is proposed that each published result should be accompanied by the specific data reduction procedures and assumptions used so that data may be compared. Preparation of plasma-sprayed ceramic samples has a significant influence on the MIP result. Sample fragmentation into irregular pieces (below about 1.2 mm effective diameter) prior to the MIP measurement resulted in an increase of surface effects such that the surface roughness dominated the MIP data and the measured porosity volume increased. Variation in sample thickness between 0.8 and 4.7 mm did not change the measured porosity. Orientation (parallel or perpendicular to the substrate) of the flat surface did not have a measurable effect on the MIP results.

1. Introduction

Mercury intrusion porosimetry (MIP) is a common technique for characterizing the porous microstructure of materials [1, 2]. Availability of commercial equipment and the wide range of applicability (with respect to materials as well as pore sizes) are the main advantages of this method for engineering practice [3]. This broad use, however, brings about problems in specific cases which may arise from the limitations of this technique.

A number of corrections on MIP results have been discussed in the literature [4–6]. These widen the use of the technique and improve the relationship between the MIP data and the void system characteristics. They may, however, also make the comparison of the MIP data obtained by different researchers difficult.

An ideal porosity measurement technique should have the following properties [7]: (i) all of the porosity should be measured; (ii) all of the pores should be characterized with respect to their volume, size, shape and surface; (iii) anisotropy of the void system should be characterized; (iv) the method should be reproducible in time and space (i.e. anytime and anywhere); (v) the measurement technique should not alter the material structure; and (vi) voids within the studied range should be measured with the same precision. There is no method currently available which satisfies all of these conditions. It is, therefore, important to state for each technique its limitations, model or models it is based on and corrections (i.e. numerical processing of data) applied. Some of the data reduction procedures may be characteristic for the technique and some may depend on the material properties or on the void system characteristics.

This paper discusses the use and limitations of the MIP technique with respect to plasma-sprayed ceramic deposits. It also studies the influence of the sample preparation procedures on the MIP result.

2. Theory
2.1. Principle

The mercury intrusion porosimetry technique consists of enclosing the sample in a chamber, evacuating and filling the chamber with mercury and applying incremental pressure on the mercury. The intruded volume of mercury is recorded together with the pressure. This results in the intrusion versus pressure curve, which may be normalized with respect to sample weight or volume. The experimental data is analysed on the basis of the Washburn equation [1, 2]:

$$d = \frac{-4\gamma\cos\theta}{p} \qquad (1)$$

---

which converts the pressure into equivalent pore sizes on the assumption of tubular pores. The term d in this equation represents the equivalent diameter of intruded pores, γ is the surface tension of mercury, θ is the angle of contact between the pore walls and mercury, and p is the pressure applied on the mercury. The equivalent diameter on current commercially available porosimeters may vary between hundreds of micrometres to a few nanometres (i.e. equivalent to pressures of 0.1 to 400 MPa, respectively), giving the MIP technique a wide range of pore size measurement [3].

The intrusion curve may be converted into a pore volume distribution as well as surface area distribution by applying a cylindrical pore model. The second method of deriving surface area is the "modelles method" [3], with no assumption of any specific pore geometry. Here the work required to force mercury into the pores ($p\,\mathrm{d}V$) is assumed to be equivalent to the work required to immerse the pores' area into the mercury ($\gamma\,\mathrm{d}S\cos\theta$). This yields an integral equation for the surface area of pores S.

2.2. Errors and data reduction procedures

Representative specimens are intruded with mercury by applying pressure in a MIP instrument. Then, the pressure and intruded volume data are converted to pore distribution data, using a theoretical model. This procedure leads to error in the final results arising from four different aspects, namely, instrumental, procedural, modelling and the specimen.

2.2.1. Instrumental

Error in the measured data [4, 8, 9] arising from the measurement method and apparatus are often neglected. The intruded volume data include the behaviour of the machine and mercury during the test [4, 6]. For example, the expansion of the machine, compressibility of mercury in the sample chamber and compression of the unintruded volume of sample. This error may be partially evaluated by carrying out an empty or dummy run; i.e. a MIP run without any sample. However, such an evaluation is not exact, since the volume of mercury in the empty run is different from the volume during the measurement. Moreover, since there is no sample in the blank run, the compressibility of the sample is neglected.

Equations have been devised, which allow corrections for most of these effects. The correction on sample compressibility is probably the most difficult part of this data analysis since the compressibility of materials may not be available. Moreover, the compressibility of materials depends on the porosity, which changes during the measurement as the pores become filled with mercury. Another effect, which may be included in this correction, is the effect of temperature changes within the chamber. These temperature changes are caused by work of mercury compression and if the cooling of the chamber is insufficient, then there may be a significant temperature increase. Mercury thermal expansion then has to be included in the data evaluation.

With the exception of the sample compressibility, these corrections are related to the available hardware (machine) and are often sufficiently small that they are not needed [9] for routine measurements. This fact may, however, become an issue for samples of low porosity since the instrumental error becomes a significant fraction of the total measurement.

During the MIP experiment, the hydrostatic pressure within the chamber changes due to a vertical pressure gradient. Depending on the construction of the porosimeter (for example, devices with vertical chambers), this pressure may be relatively high. This effect will be most significant at small pressures when it may be necessary to apply corrections. The importance of this correction depends on the machine construction and is often taken into account during the data reduction procedures [9].

2.2.2. Procedural

In the MIP procedure, the values of contact angle and surface tension are usually considered to be constant and not material dependent [6, 10, 11]. Often used values for contact angle vary between 117 and 140 degrees. Surface tension values usually vary between 0.473 and 0.484 N m^{-1}; however, they vary not only with the sample material but also with the mercury purity. Both values influence the calculated pore size (Equation 1) and, therefore, shift horizontally the intrusion versus effective pore size curve to different pore diameters.

The surface tension of the mercury depends on the pore size being measured, thus it varies during the experimental run [11]. Some workers [6, 10] have also shown that there may be different mercury surface tensions for intrusion and extrusion runs, resulting in the difference between intrusion and extrusion curves of identical specimens [6, 10]. The surface tension effect can be corrected if the surface tension of mercury is known for a planar mercury surface (infinite curvature). Surface tension of mercury is regularly measured using large surface curvatures and this data is used to correct the MIP data.

2.2.3. Modelling

Evaluation of the intrusion curve assumes a void structure consisting of individual cylindrical pores. However, the actual pore structure forms a complex pattern of shapes and sizes, and its evaluation is complicated by pore connectivity, bottle ink pores, delayed intrusion, etc.; factors generally related to the microstructure. Different methods have been devised to cope with these problems. Many of these effects were modelled and shown to result mostly in a shift of the size distribution [12–14] but with limited effect on the total volume of porosity.

A cylindrical pore shape is assumed in the original Washburn equation. This equation may be generalized for other pore shapes [5, 15]:

$$d = \frac{-\phi\gamma}{p}\sin(\alpha + \theta) \qquad (2)$$

The term ϕ is the shape factor (Table I) and α is the angle of the walls of the intruded pore as defined in Fig. 1. Generally, the shape factor for any pore shape should be between 2 and 4. On top of this geometrical pore shape effect, the effective contact angle changes depending on the local angle α of the walls and the axis of the pore (Fig. 1). Thus even though Equation 2 is relatively simple, the pores need to be uniform in shape to enable this correction to be applied.

2.2.4. Specimen
If the MIP sample volume is large, some of the internal pores will not be intruded by mercury even at high pressures [16]. Hence, MIP samples, in general, are prepared from large specimens by fragmentation. This sample preparation procedure leads to two possible effects. The first is a possible increase of the void fraction due to formation of new cracks within the material and the second is opening of any originally closed porosity. Both of these effects result in an increase of the pore volume.

It is possible to avoid fracturing of specimens by cutting the specimens into discs or plates, and thereby avoid formation of new cracks. This is a convenient form while studying deposits and ribbons. Again, if the thickness of the disc or ribbon is large, a part of the void microstructure may not be accessible for the mercury.

Sample sectioning is not usually considered a problem. However, many specimens, such as plasma-sprayed ceramic deposits, contain complex void systems with several types of voids which are organized in an anisotropic way [17–20]. In sprayed deposits, there are two major void systems within the microstructure; namely, interlamellar pores which are mostly parallel with the substrate and intralamellar cracks within lamellae which are mostly perpendicular to the substrate. Samples with such oriented defects will have different void systems terminating on the surface. If these void systems are of different sizes, they can result in different mercury paths for samples and lead to a variation in the results.

2.3. Summary
Errors from a number of sources influence the microstructural view that is perceived by a MIP test. It has been shown that depending on the material, sample size, total porosity and pore sizes, these changes may be up to 45% of the porosity volume (for low porosity samples) and up to 40% change in the pore size [4]. Such extreme corrections may occur only in a limited number of cases, however, they should always be considered.

As noted above, instrument errors can be minimized by design of the hardware and software, and the data reduction procedures can be built into the system software. Procedural errors (surface tension and contact angle) are normally considered negligible and ignored [6, 10, 11] in routine measurements.

Most of the measurements are performed at conventional, known evaluation parameters; such as con-

TABLE I The shape factors for Equation 2 [4]

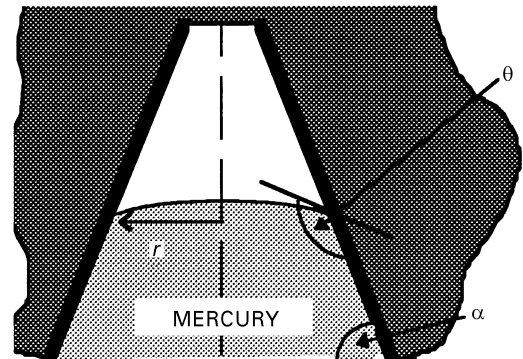| Pore cross-section	ϕ
Circular	4.00
Elliptical with aspect ratio 1.5	3.37
Elliptical with aspect ratio 4	2.73
Elliptical with aspect ratio 16	2.56
Slit (parallel walls)	2.00

Figure 1 Geometry of intruded mercury into the non-cylindrical pore (cone) with the angle between the base and walls being α.

stant contact angle $\theta = 140°$, and constant surface tension $\gamma = 0.480 \text{ N m}^{-1}$ with $\phi = 4$. Though many workers have concentrated on the errors and corrections due to modelling, it is impractical to apply the correction for different void shapes on systems with complex void shapes. There have also been some suggestions to use $\phi = 3$ instead of 4 as the more realistic value for complex shapes [4] in Equation 2. However, for the sake of comparing results, the ϕ value used should be based on general agreement and the value of 4 (i.e. circular pore cross-section) is often used. It is important to understand that the calculated MIP pore sizes may be as much as twice the real pore dimensions in the extreme case of pores which are shaped as slits. Errors arising from the size and sectioning of samples with complex void structures vary with different materials and require to be experimentally evaluated. The influence of sample sizes and sample sectioning on the measured data is studied in this work.

3. Experiments
3.1. Specimens and experimental procedure
Plasma sprayed alumina–titania (3 wt %) free standing forms, prepared with a water-stabilized plasma spray system (Model PAL 160, Institute of Plasma Research, Prague), were used throughout this work. These samples were prepared with porosities of about 5% (as measured by MIP and water immersion techniques [19]). The material density of these deposits (mostly composed of gamma alumina) was about 3.65 g cm^{-3} [19].

A commercially available MIP system (Autoscan 33, Quantachrome Corp., FL) was used to measure the pore size distribution of specimens. System-supplied software programs (version 3.0) were used for data collection and analysis. Conventional parameter

values such as a constant contact angle $\theta = 140°$, constant surface tension $\gamma = 0.480 \, \mathrm{N \, m^{-1}}$ and $\phi = 4$ were used throughout this work. No corrections for sample compressibility and mercury compressibility were made. The corrections for an empty run and other factors were not carried out as these are built into the system.

Pressure and intruded volume data were recorded in the range of 2 to 33 000 PSIA (0.01 to 228 MPa, respectively), corresponding to the pore sizes of 100 μm to 3 nm diameter. Off-line programs were used to obtain the pore size distribution as well as bulk properties such as bulk density, apparent density, total intruded volume ($\mathrm{cc \, g^{-1}}$) and total surface area ($\mathrm{m^2 \, g^{-1}}$). Intrusion statistical data including mean, mode and median values of pore volume, surface and number fractions were also calculated. Variation in the pore size distribution, bulk properties and the intrusion statistics as a function of experimental variables was used to study the effect of the parameter on the MIP results.

3.2. Experimental objectives

Three experiments were performed to study the three sample effects. The influence of sample size for randomly shaped samples was carried out to establish the optimum sample size. The influence of sample thickness was studied to estimate the depth of penetration of the mercury during MIP and, therefore, indicate the maximum thickness of the deposits that can be fully characterized. The influence of the sample sectioning was studied to establish the effect of the orientation of the sample intrusion face (parallel or perpendicular to the substrate) on the measured void structure. This experiment was performed to examine whether the MIP results of an anisotropic specimen are influenced by the sample sectioning procedure.

3.3. Preparation of MIP sample pieces

The samples for the size experiment were prepared by fracturing a deposit of $\sim 3 \, \mathrm{cm} \times 3 \, \mathrm{cm} \times 0.5 \, \mathrm{cm}$ into smaller particles. These smaller particles were divided into six size categories and average particle size was calculated in the following manner:

(a) For the four largest size categories the particles were manually counted, weighed and the average weight calculated. Using the density of gamma alumina (3.65 g cm^{-3} [19]) average particle volumes in each size category were calculated and, assuming the particles to be spheres, average diameters in each category were established.

(b) The two size categories with the smallest pieces were sieved and the sieve opening was used as an approximation of the average particle diameter. The average particle diameters varied from about 5.5 to about 0.1 mm.

Samples of varying thickness were cut in the form of wafers with the cuts being perpendicular to the substrate. Plate specimens of dimensions 25 mm ×

5.2 mm × t mm, where t varied (0.8, 2.0 and 4.6 mm), were sectioned and these samples were used for specimen thickness studies.

Sets of two samples of dimensions 25 mm × 5 mm × 1.0 mm were cut into wafers for sample sectioning studies. The large sample surface was oriented on one sample parallel to the substrate surface (in-plane sample) and perpendicular to the substrate surface on the other sample (cross-section sample).

4. Results and discussion
4.1. Influence of sample size

For further discussion some terms need to be defined and their meaning clarified. Mercury intrusion porosimetry yields a specific pore surface area, i.e. surface area of the intruded voids, and this is generally assumed to be equal to the internal surface of the sample particles. The discussion in this paper needs definition of another similar term, specific particle surface area, which represents the specific surface area of the sample particles, i.e. only the external surface of these particles. Such data for randomly shaped particles is difficult to obtain, therefore it is approximated by the surface of the spheres; assuming that the particles within one size category are all of the average particle diameter calculated during scaling. It should be noted that this approximation yields lower values than the true surface area.

The results are presented in Table II and Figs 2 and 3. The standard error of the MIP result represents statistical reproducibility established by multiple measurement of the samples with similarly sized and shaped particles prepared from the one large deposit.

The results of the experiment with varying average particle diameter show that the porosity values measured on smaller diameter samples are high. Independent water immersion results of the large samples revealed that they could not contain more porosity than about 6–7%. However, for samples with an average particle diameter of 1.2 mm and smaller, the MIP porosity volume increased and reached unrealistic values of 37% for a sample with 0.1 mm average diameter particles. This suggests that there is another mechanism which generates such porosity values. Table II and Fig. 2 suggest that the increase in the porosity and specific particle surface area are related,

TABLE II Influence of sample size on MIP results. For detailed explanation of terms specific pore surface area and specific particle surface area see text

Effective diameter (mm)	Specific particle surface area of the specimen (cm^2 cm^{-3})	Porosity volume (0.5) (%)	MIP specific pore surface area (0.8) (10^3 cm^2 cm^{-3})
5.5	10.9	5.9	16.2
3.1	17.5	5.3	13.3
2.2	26.8	5.9	13.7
1.2	47.4	6.6	12.2
0.5	120.0	12.8	10.8
0.1	600.0	37.4	9.0

Note: The values in brackets are standard uncertainties established from statistical evaluation of multiple measurements.
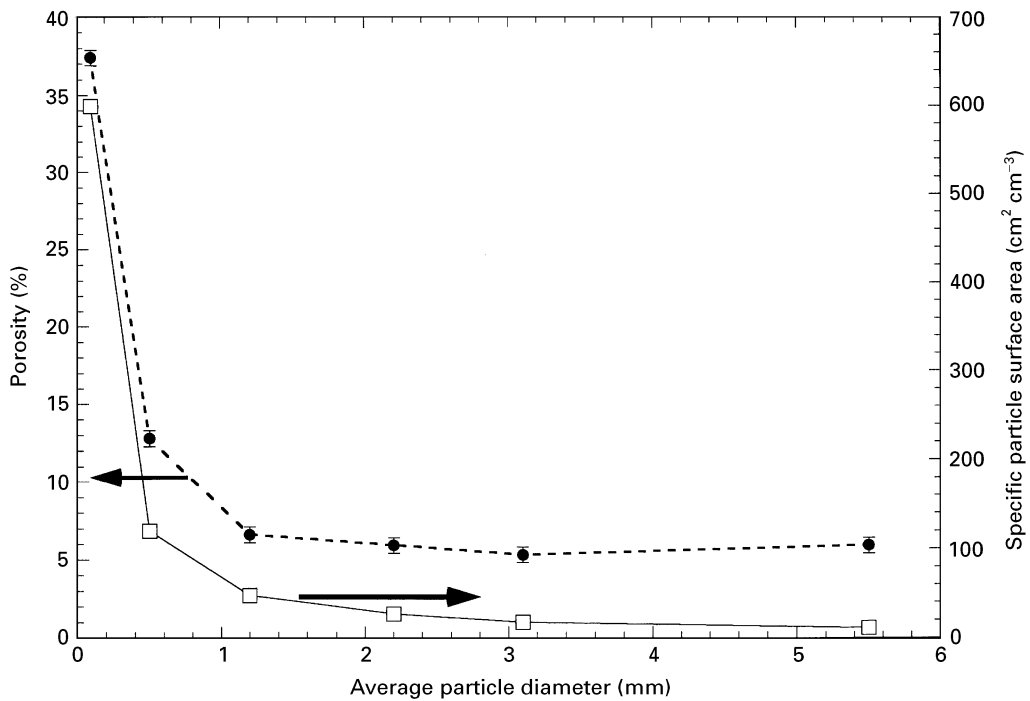
3928

Figure 2 Porosity volume (– – ● – –) and specific particle surface area (—□—) dependence on the average particle diameter.
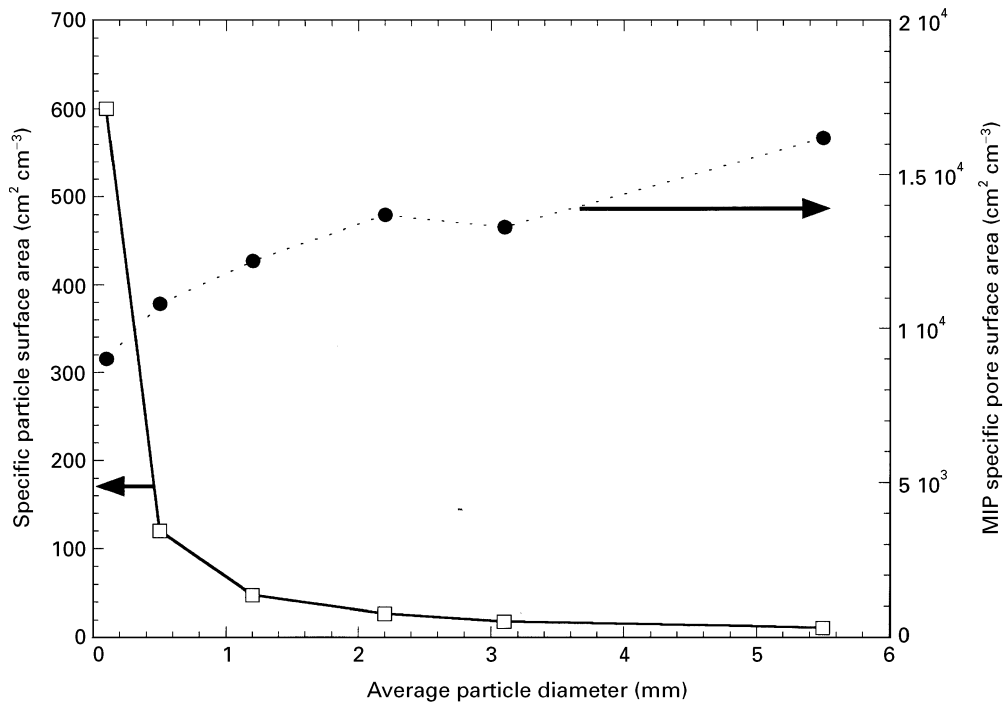

Figure 3 Specific particle surface area (—□—) and MIP specific pore surface area (– – ● – –) dependence on the average particle diameter.

most likely through the surface roughness. The surface roughness is always included in the porosity in the MIP measurement. Therefore, as the sample surface increases, the associated volume of surface roughness increases. At some point the contribution from the surface roughness may become appreciable and eventually even more significant than the internal porosity.

These data may also be used to estimate the average height of the surface roughness for the samples and compare it with the features known to be present in the microstructure. For the sample with smallest particles (average particle diameter 0.1 mm) the MIP measured porosity was about 37%. Assuming that the internal porosity is equivalent to the porosity of the samples with large particles (about 6%), about 31% porosity can be related to this surface effect. Assuming a sphere of 100 μm diameter, about 10 μm high peaks on the surface are necessary to produce this porosity. Since the spherical shape is an idealization with minimum surface area compared to the real particle surface the real surface roughness is likely to be lower than this estimate. This estimate of surface roughness agrees reasonably well with the splat thickness of these deposits which is about 5 μm.

Dependence of the MIP measured specific pore surface area on average particle diameter is compared in Fig. 3, together with the specific particle surface area. This figure shows, that the specific pore surface area decreases with the decrease in the average particle diameter. Thus, newly formed voids must be of larger size than the original pores. This is confirmed by the pore size distributions, Fig. 4, measured by MIP which change from a distribution of ~0.1–0.4 μm for large particle size samples to significantly larger pore sizes of ~10–100 μm for small particle size samples.

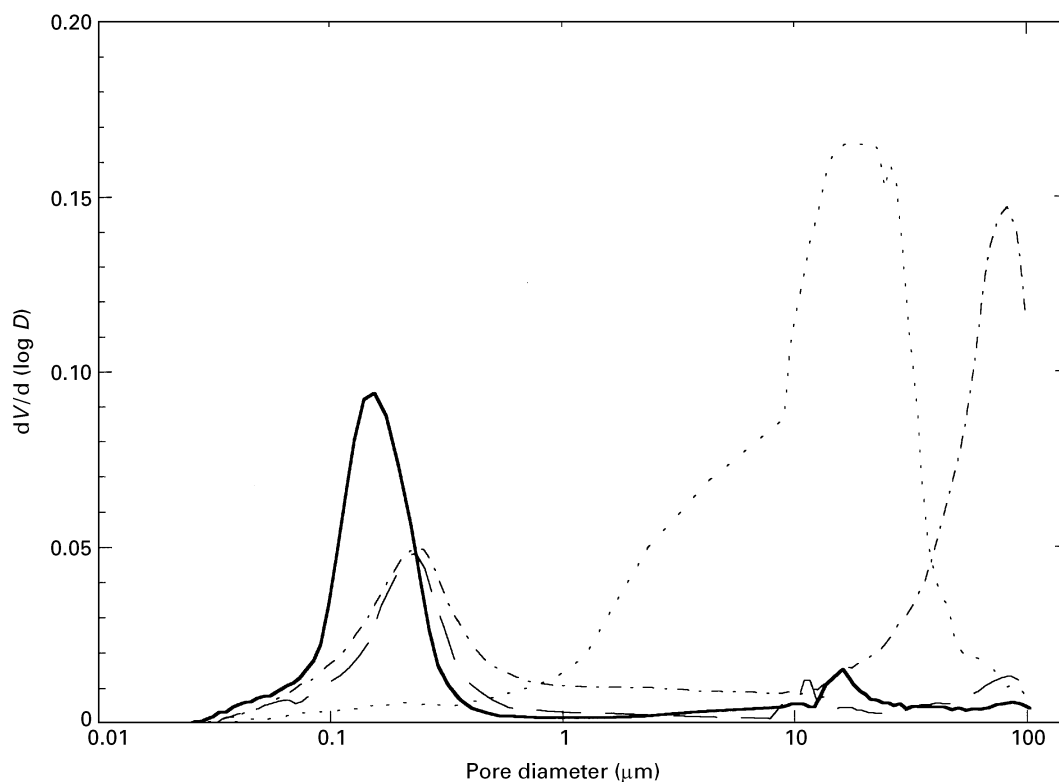Thus, the low porosity sample MIP data are dominated by the surface roughness at an average particle

Figure 4 Dependence of the MIP pore diameter distribution on the average particle diameter: —— 5.5 mm, — — 1.2 mm, — – – — 0.5 mm and -- -- -- 0.1 mm average particle diameter.
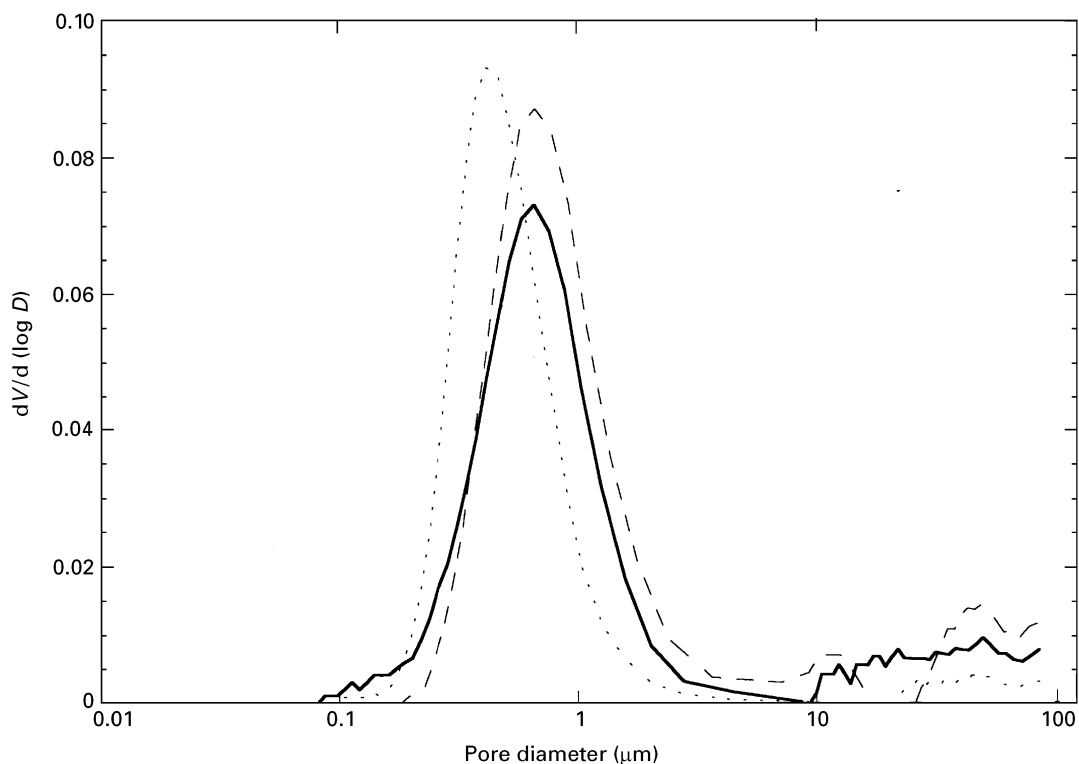

Figure 5 Dependence of the MIP pore diameter distribution on the sample thickness (– 0.8 mm, – – – 2.0 mm and - - - - - 4.6 mm).

3930

diameter of ~1.2 mm. Below this diameter, the MIP measurements do not represent the internal porosity of the deposit. The character of voids in these measurements changes due to the preparation of the smaller sample particles. The fracture scanning electron microscopy (SEM) micrographs show large fractured splats resembling large "cliffs", which could be locations of narrow cracks within the lamellae [20, 21]. These narrow cracks dominate the large particle size samples and, as the sample is further comminuted, fracture steps in increments of splat height form larger sized voids (i.e. surface roughness) on the surface of the particles.

4.2. Influence of sample thickness

Fig. 5 presents the pore size distribution of samples with different thickness. In the studied range of thickness (0.8, 2.0 and 4.6 mm) there was no change in the results of MIP porosity and density. All three samples showed MIP porosity varying from 4.95 to 5.30%, with no monotonic dependence on the thickness. The statistical error of these measurements was estimated to be ~0.5%. The density results varied between 3.35

TABLE III MIP data obtained on specimens with different orientations (the values of standard uncertainties are estimated in brackets)

Specimen orientation	Porosity volume (%) (0.5)	Density (g cm^{-3}) (0.03)
In-plane	5.6	3.45
Cross-section	5.8	3.48

to 3.38 g cm^{-3} for apparent (as-received) density and 3.50 to 3.55 g cm^{-3} for residual density. The standard uncertainty of the density measurements was estimated to be about 0.03 g cm^{-3}.

4.3. Influence of sample sectioning

Table III presents the results of MIP measurements carried out on specimens cut at different orientations. The intrusion volumes of open porosity and density (Fig. 6) were, within the margin of errors, the same.

The experiment did not show different results for the samples prepared as plates with large surface areas parallel and perpendicular to the substrate, indicating that either (i) both void systems have the same void sizes or (ii) the two void systems are interconnected. Since previous work [20] has revealed that the two void systems have different sizes of voids, the MIP results infer that these void systems are interconnected. The results suggest that the MIP technique cannot be used to map the anisotropy of a sprayed specimen. However, the results also indicate that, due to inter-connection between the void systems, the specimen sectioning procedure does not affect the MIP result.

5. Concluding remarks

The study of limitations and model assumptions of the MIP technique shows that the relationship of MIP data to the pore structure is complex, especially in the case of void systems with complex shapes and anisotropy. Many data reduction procedures have been developed to improve this relationship. The need for these data reduction procedures varies depending on
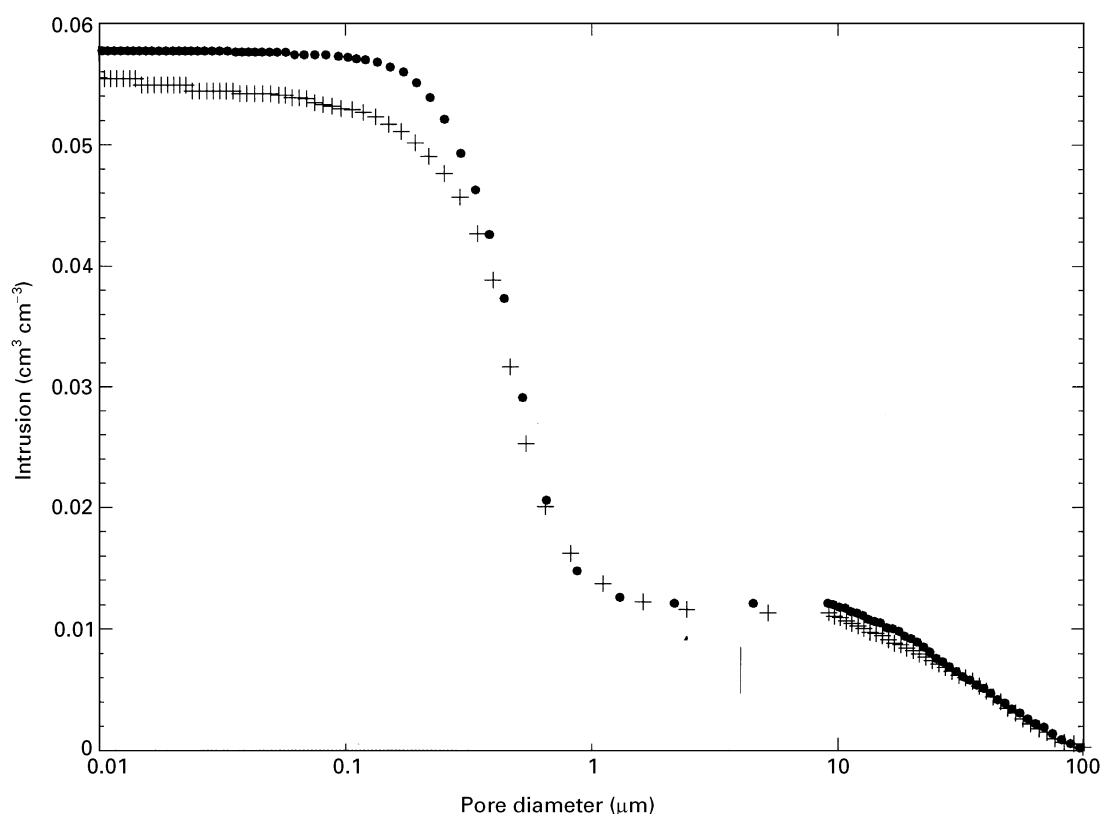

Figure 6 Dependence of intrusion curve on the intrusion face of the sample (+ face parallel with substrate and ● face perpendicular to substrate).

the available hardware (porosimeter) and on the measured characteristics of the pores.

Most of the data reduction procedures may not be required for routine engineering practice. However, conditions of the measurement and data evaluation should be clearly stated, and the possible influence of these data reduction procedures must be considered during the analysis of the results.

For irregular shaped specimens, smaller (<1.2 mm) sized samples showed increased porosity volumes (up to 37%) which could be related to the surface porosity (i.e. surface roughness). Such an effect was not observed for thin, wafer samples with thickness of 0.8 mm, since the surface of the sample and the volume of surface porosity were negligible compared to the volume of the specimen pores.

The MIP results of wafer samples with varying thickness showed that, for thickness between 0.8 and 4.6 mm, there is no significant difference in the measured porosity volumes, suggesting that the amount of porosity characterized during a MIP measurement does not depend on the sample thickness. Residual density measurement showed that the mercury could not penetrate all the pores at these sample thicknesses.

In summary, MIP measurements on plasma-sprayed ceramic deposits yield reliable and reproducible information if the sample surface area is small, i.e. the samples are in the form of wafers (layers) with sufficient thickness (~0.8 mm) or are in randomly shaped form with sufficient size (>1.2 mm equivalent diameter). A decrease in the size of randomly shaped pieces results in an increase in the measured porosity volume and, therefore, this sample preparation artefact may lead to an ambiguous understanding of the material.

References
1. S. J. GREGG and K. S. W. SING, in "Adsorption, surface area and porosity" (Academic Press, London, 1982) p. 173.
2. S. LOWELL, in "Introduction to powder surface area" (John Willey & Sons, New York, 1979).
3. T. ALLEN, in "Particle size measurement" (Chapman and Hall, New York, 1990) p. 653.
4. R. A. COOK and K. C. HOVER, *Amer. Concr. Inst. Mater. J.* **91** (1994) 152.
5. O. Z. CEBECI, *J. Colloid Interface Sci.* **78** (1980) 383.
6. J. KLOUBEK, *ibid.* **1** (1994) 10.
7. D. H. EVERETT, *Charact. Porous Solids* **39** (1988) 1.
8. D. N. WINSLOW, *J. Colloid Interface Sci.* **67** (1978) 42.
9. S. LOWELL and J. E. SHIELDS, *Powder Technol.* **28** (1981) 201.
10. R. W. SMITHWICK and E. L. FULLER Jr, *ibid.* **38** (1984) 165.
11. J. KLOUBEK, *ibid.* **29** (1981) 63.
12. D. K. EFREMOV and V. B. FENELONOV, *Kinet. Catal.* **34** (1993) 625.
13. H. H. D. LEE, *J. Amer. Ceram. Soc.* **73** (1990) 2309.
14. D. M. SMITH, D. P. GALLEGOS and D. L. STERMER, *Powder Technol.* **53** (1987) 11.
15. R. G. JENKINS and M. B. RAO, *ibid.* **38** (1984) 177.
16. C. C. BARTENEV, *Obmen Opytom Inf.* (*Exchange of experience and information*) **11** (1976) 98 [in Russian].
17. P. EXNAR, *Ceramics-Silikaty* **38** (1994) 16.
18. J. ILAVSKY, A. J. ALLEN, G. G. LONG, S. KRUEGER, H. HERMAN, C. C. BERNDT and A. N. GOLAND, in "Proceedings of the 14th International Thermal Spray Conference", Kobe, Japan, May 1995, edited by A. Ohmori (High Temperature Society of Japan, Osaka, 1995) p. 483.
19. J. ILAVSKY, PhD dissertation, State University of New York at Stony Brook, USA (1994).
20. A. HADDADI, F. NARDOU, A. GRIMAUD and P. FAUCHAIS, in "1995 Advances in Thermal Spray Science and Technology", edited by C. C. Berndt and S. Sampath (ASM International, Materials Park, OH, 1995) p. 249.
21. R. Mc PHERSON, in "Proceedings of 5th Conference on Aluminium Oxide", Prague, Cechoslovakia, August 1990, edited by V. Brozek and V. Rene (Czechoslovak Science and Technical Society, Prague, 1990) p. 42.